

This is the **accepted version** of the journal article:

Lopez-Soriano, Sergio; Parrón Granados, Josep. «Performance assessment of a novel miniaturized RFID tag for inventorying and tracking metallic tools». IEEE journal of radio frequency identification, Vol. 2, Issue 3 (September 2018), p. 127-133. DOI 10.1109/JRFID.2018.2868780

This version is available at <https://ddd.uab.cat/record/274027>

under the terms of the  ^{IN}COPYRIGHT license

Performance Assessment of a Novel Miniaturized RFID Tag for Inventorying and Tracking Metallic Tools

S. Lopez-Soriano and Josep Parron

Universitat Autònoma de Barcelona, Bellaterra, Spain, sergio.lopez.soriano@uab.es

Abstract—This contribution proposes a novel RFID tag antenna operating in the EU UHF band (865-868 MHz). Miniaturization techniques have been used to achieve a reduced volume ($20 \times 2.56 \times 3 \text{ mm}^3$) in order to make it suitable for labelling metallic tools. Simulations are used to assess the tag performance when operating on tools of different sizes. These simulations are validated through measurements in a reference scenario (anechoic chamber). Finally, a real scenario (tool hanging board) is considered in order to evaluate tag performance when interacting with other tags and tools.

Index Terms—antenna design, RFID tags, metallic objects, tool tagging, UHF RFID system performance.

I. INTRODUCTION

Nowadays, the use of the RFID (Radio Frequency Identification) technology for inventorying and tracking tools is of great interest in many sectors like construction, healthcare or industry [1]-[4]. Obviously, the cost of replacing lost tools has a negative impact on the profit account. However, this impact can be even more important if the project, service or production is delayed or stopped because the right tool is not at the right place at the right moment. Besides, tools accidentally left in inappropriate places can cause significant damages or, even worse, compromise safety or health.

In the case of tools, the use of conventional UHF RFID tags for metallic objects [5]-[7] is not always feasible because of the strict size, **low profile**, and shape restrictions the tag is submitted to. Accordingly, achieving a highly miniaturized tag antenna, while maintaining the required read range, is one of the toughest challenges that the designer must face. In addition, small tools are typically organized in toolboxes, work benches or tool hanging boards where they are close to other metallic objects which can impair the antenna performance, therefore, the operating environment should be also considered in the evaluation of the tag.

Antenna designs for tags with a cross section smaller than $3 \times 3 \text{ mm}$, suitable for labelling metallic tools, have not been reported previously in the literature to the best of the authors' knowledge. Although there are commercial solutions with **reduced** cross-sections that provide read ranges from 1 to 3 meters depending on the tag length [8],

[9], no details are given in datasheets about the tool or the scenario where that performance was evaluated.

The design proposed in this contribution is based in the short-ended coupled patches presented in [10] (volume $65 \times 20 \times 1.5 \text{ mm}^3$). A second version of this antenna was reported in [11] with a smaller footprint at the expense of increased thickness (volume: $32 \times 18 \times 3.2 \text{ mm}^3$). Other contributions that made use of short-ended coupled patches [12]-[14] did not reduce the antenna volume any further, so none of these solutions is suitable for our application.

In this report, a very important size reduction is achieved through a multilayer technique presented in [15] for reducing the physical length of a planar inverted-F antenna (PIFA). The present article investigates the application of this technique to a symmetrical structure [10].

Next, section II will be devoted to the design of a highly miniaturized tag antenna that can be attached to different metallic tools. The performance of the tag on different metallic plates will be assessed through simulations in section III. After manufacturing and experimentally validating the design in a reference scenario (section IV), we will evaluate the performance in a real scenario with multiple tools (section V).

II. ANTENNA DESIGN

A. Antenna geometry and miniaturization

The proposed design consists of two coupled short-ended patches that have been folded to achieve the desired size. Fig. 1 shows the antenna 3D view and the main geometric parameters for the case of a 4-layer structure.

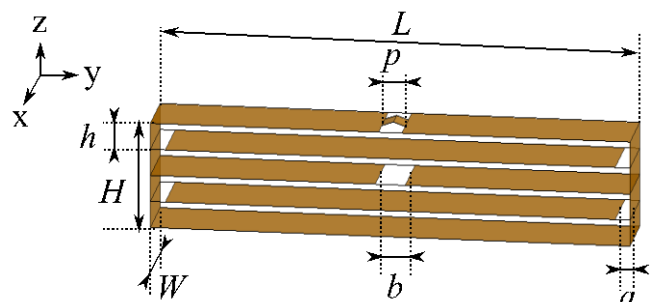


Fig. 1: Antenna 3D view of a 4-layer structure.

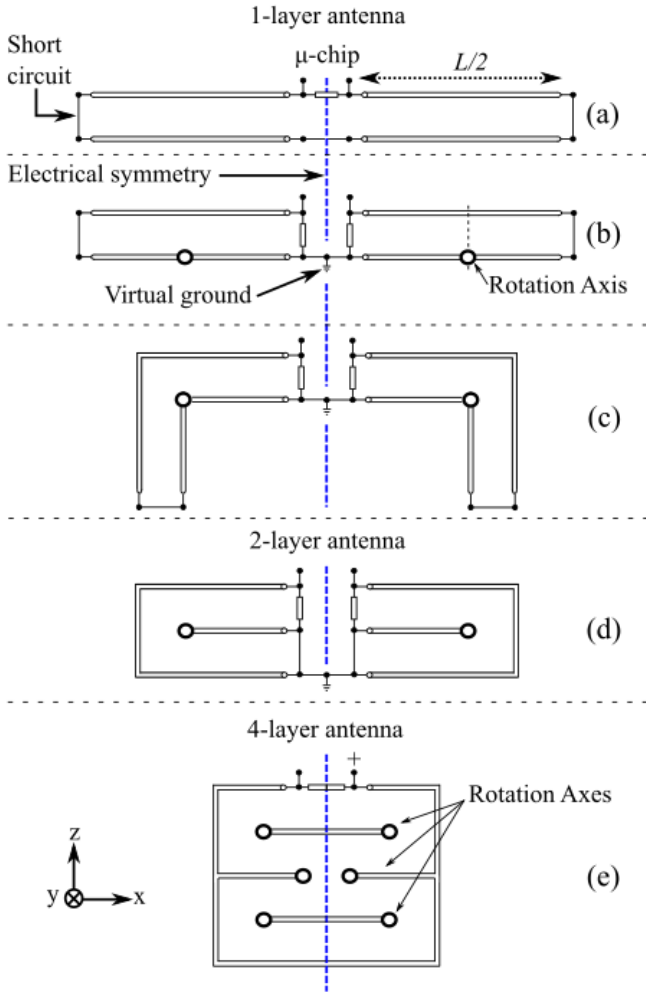


Fig. 2: Miniaturization procedure.

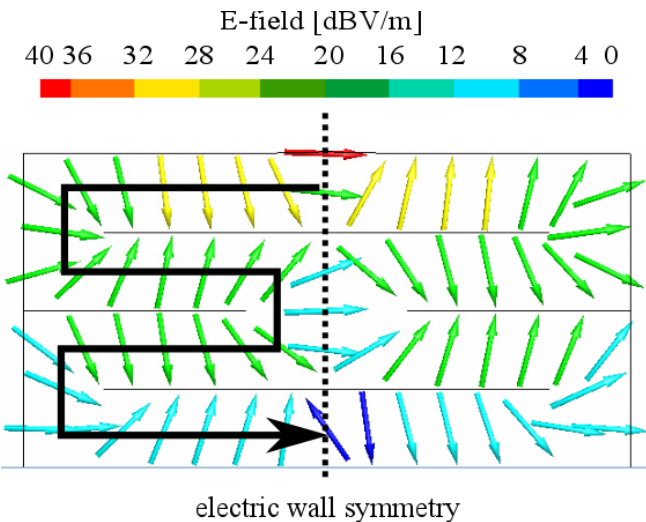


Fig. 3: Distribution of electric fields inside a 4-layers antenna.

Unlike in [15], where the length reduction was accompanied by an increase of the antenna thickness, in our case, we keep the thickness smaller than 3 mm, in order to match the low profile required by the application. The width of the antenna has been further reduced ($W = 3$ mm) in order to fit the application requirements. Accordingly, the overall antenna volume has been drastically reduced compared to [10]-[14].

Fig. 2 describes the miniaturization procedure. The shorted-ended coupled patches can be modelled as a two short-ended transmission lines in series (Fig. 2.a) [14]. Fig. 2.b to Fig. 2.d show as the transmission line is folded to achieve a 2-layer structure with a smaller total length. This operation can be repeated to achieve further length reduction (Fig. 2.e).

Fig. 3 shows the electric field distribution inside the folded structure, which corresponds to the distribution of two straight short circuited transmission lines. Therefore, for given values of W , H and h , the chip capacitive reactance is compensated by adjusting the antenna length L . Once L is fixed, the input resistance will mainly depend on the losses of the chosen dielectric substrate so it cannot be tuned easily.

B. Simulations

In order to evaluate the degree of miniaturization that can be achieved with the proposed structure we simulated several designs (with the same values of $W = 3$ mm and $H = 3.1$ mm) with different number of layers ($N = H/h$). The antennas are designed to operate in the UHF European band (865-868 MHz). The input impedance must be complex conjugate matched to the Alien Higgs-4 (AH4) microchip ($Z_{IC} = 20 - j191 \Omega$ at 867 MHz) [16].

Arlon AD1000 ($\epsilon_r = 10.2$, $\tan\delta = 0.0023$) [17] substrate is selected, due to its high relative permittivity, in order to achieve additional miniaturization. Simulations are carried with simulation software FEKO [18] placing the antenna over an infinite ground plane.

Once we obtain the simulated power transmission coefficient (τ) [19] and the gain (G) for the normal direction (z -axis), the theoretical read range (Rr) can be computed as [19]

$$Rr = \frac{\lambda}{4\pi} \sqrt{\frac{EIRP \chi_p G \tau}{P_s}} \quad (1)$$

where λ is the free space wavelength, $EIRP$ is the equivalent isotropic radiated power (3.28 W according to European regulations), χ_p is the polarization mismatch between the reader antenna and the tag antenna (0.5 for a linearly polarized tag antenna) and P_s is the AH4 sensitivity (-20.5 dBm). The product $G\tau$ is also known as the realized gain and will be considered the main figure of merit of our antenna.

Table I summarizes the results of the study. We can see that increasing the number of layers does not produce a significant length reduction unless $N \geq 4$. On the other hand,

increasing N results in a reduction of $G\tau$ and Rr due to the substrate losses, therefore, we decided to use $N = 4$ as a compromise between miniaturization and read range.

Since the thickness of the AD1000 slab available in our lab is 0.64 mm, we had to redesign the antenna taking into account that restriction. For sake of comparison with most results in literature [5], we also considered that the object to label was a metal plate of 20 x 20 cm². The final dimensions of the proposed antenna are collected in table II.

TABLE I. SIMULATED ANTENNA PERFORMANCE FOR DIFFERENT NUMBER OF LAYERS (N). ANTENNA SUBSTRATE AD1000, $W = 3$ mm AND $H = 3.1$ mm.

$N=H/h$	h (mm)	L (mm)	$G\tau$ (dB)	Rr (m)
1	3.1	47.0	-9.1	4.4
2	1.55	33.5	-9.4	4.3
4	0.77	19.8	-9.9	4
8	0.38	10.1	-12.3	3.4
16	0.19	5.1	-14.8	2.6

TABLE II. ANTENNA FINAL DIMENSIONS (IN mm)

L	H	W	h	p	a	b
20.5	2.56	3	0.64	1	1.28	0.64

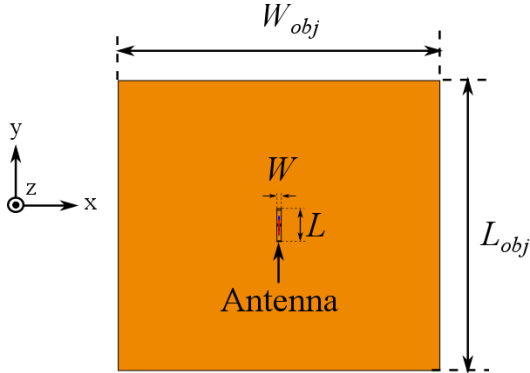


Fig. 4: Position of the tag over the metallic object.

III. EFFECTS OF THE SIZE OF THE METALLIC OBJECT IN THE TAG PERFORMANCE

In this section we assess, through simulations, the performance of the proposed tag when it is placed on the center of metallic plates with different dimensions $L_{obj} \times W_{obj}$ (Fig. 4).

We start by setting $L_{obj} = 20$ cm and sweeping dimension W_{obj} , Fig. 5 shows the simulated realized gain. It can be seen that the **realized gain of the 20 x 20 cm² metallic plate is only 2.5 dB better than the infinite ground plane**. However, the narrower the plate is, the better the realized gain. Fig. 6 shows that this behavior is mainly due to the improvement of the radiation efficiency when W_{obj} decreases.

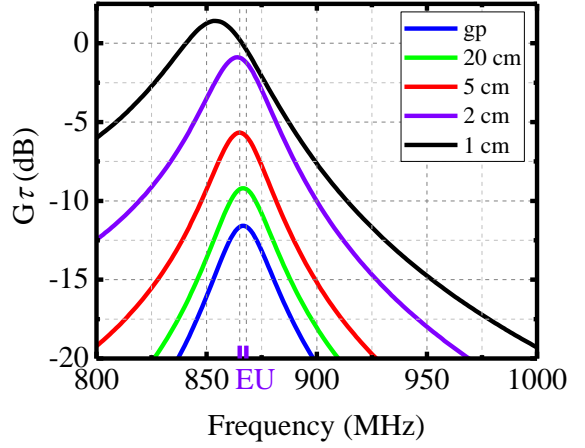


Fig. 5: Simulated realized gain along z-axis for the proposed tag over metallic plates with $L_{obj} = 20$ cm and different W_{obj} values. An infinite ground plane (gp) has been included as a reference.

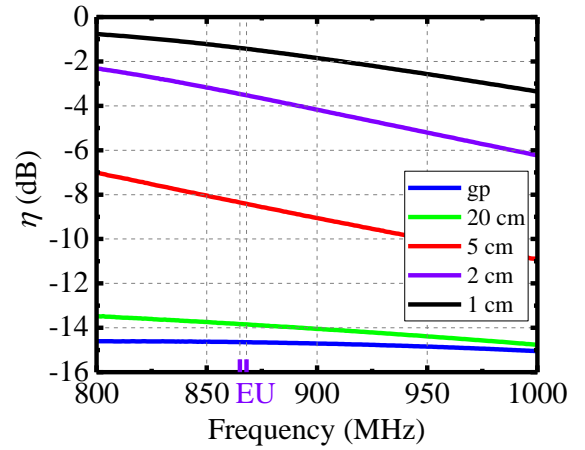


Fig. 6: Simulated radiation efficiency for the proposed tag over metallic plates with $L_{obj} = 20$ cm and different W_{obj} values. An infinite ground plane (gp) has been included as a reference.

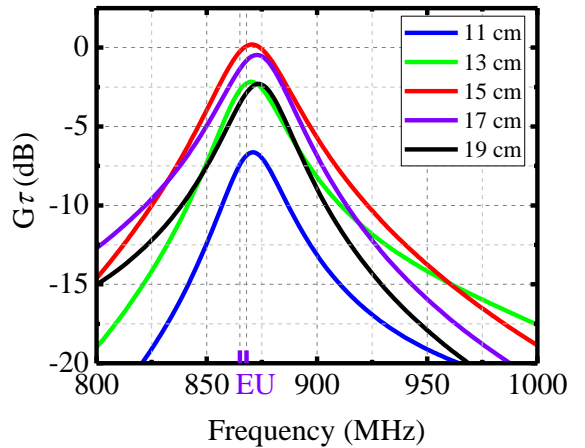
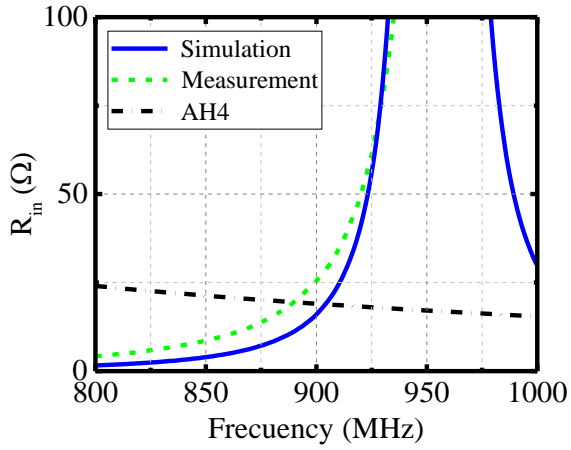


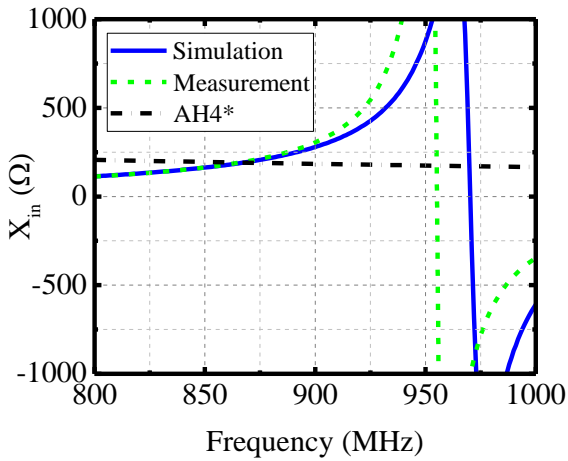
Fig. 7: Simulated realized gain along z-axis for the proposed tag over metallic plates with $W_{obj} = 2$ cm and different L_{obj} values.



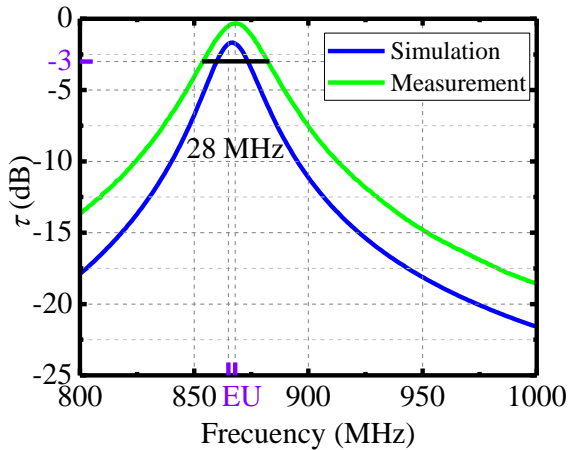
Fig. 8: 4-layer tag prototype.



(a)



(b)



(c)

Fig. 9: Antenna input impedance. a) Resistance. b) Reactance. c) Power transmission coefficient for AH4 chip.

Obviously, variations in the antenna power transmission coefficient due to the plate size also play a role in the realized gain. Nevertheless, they can be considered a second order factor unless the object becomes very narrow. In this case, there is a slight shift of the maximum realized gain towards low frequencies (Fig. 5) that should be corrected by decreasing the antenna length L .

Next, since we are interested in labelling tools, we set $W_{obj} = 2$ cm and sweep parameter L_{obj} . Results plotted in Fig. 7 show that the maximum realized gain is achieved for the length that causes the metallic plate to be resonant at the EU UHF RFID band.

IV. ANECHOIC CHAMBER MEASUREMENTS

A first prototype was fabricated using the dimensions of Table II (Fig. 8). Then, we measured the performance of the tag in a controlled environment (anechoic chamber) in order to compare with simulations.

A. Input impedance

The input impedance measurement of the balanced antenna was carried using the setup proposed in [20]. The tag was placed on a metallic plate of 20×20 cm².

Fig. 9 compares the simulated and measured input impedance. The measured input resistance (Fig. 9.a) is higher than the simulated, probably due to the additional losses introduced in the manufacturing process. In any case, the best matching is achieved in EU UHF band when the antenna reactance compensates the chip reactance (Fig. 9.b). Additional losses improve the measured power transmission coefficient (Fig. 9.c) with respect to the simulation. However, we also expect a decrease of the measured gain.

B. Realized gain and read range

The turn-on power (P_{to}) of the tag was measured using the set-up shown in Fig. 10 consisting of a commercial R220 reader from Impinj [21] connected to an **antenna with a gain of 8.5 dBic** [22].

Once P_{to} was measured, the realized gain ($G\tau$) was calculated as

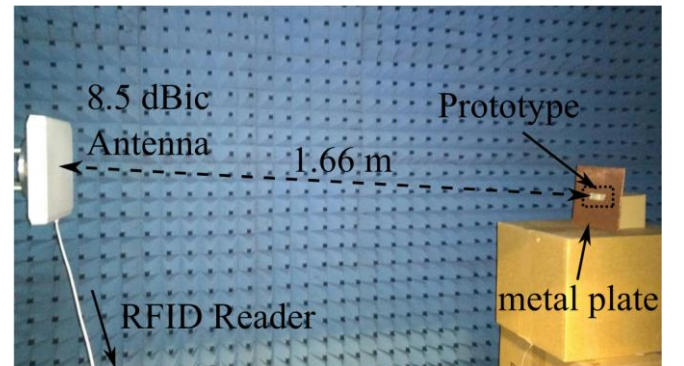


Fig. 10: Turn-on power measurement set-up.

$$G\tau = \left(\frac{4\pi r}{\lambda} \right)^2 \frac{P_s}{P_{to} G_R \chi_p} \quad (2)$$

where G_R is the gain of the antenna connected to the RFID reader and r is the distance between antennas. Again, the polarization mismatch between antennas (χ_p) is supposed to be 0.5. Next, the read range was computed using (1). Table III summarizes the results obtained for several metal plates with $L_{obj} = 20$ cm and different W_{obj} .

TABLE III. MEASURED TURN-ON POWER AND COMPUTED REALIZED GAIN AND READ RANGE

W_{obj} (cm)	P_{to} (dBm)	$G\tau$ (dB)	R_r (m)
20	25	-11.4	3.3
5	23.5	-9.9	4
2	17	-3.4	8.5
1	14.5	-0.9	11.2

The **computed** values of the realized gain were 2-3 dB lower than those obtained in simulations (Fig. 5). This difference can be attributed to the losses that were observed in measurements of Fig. 9. Overall, the trend of the realized gain agrees with the simulated results of Fig. 5.

In terms of read range, our design performs better, with a higher degree of miniaturization, than **those** designs reported in the state of art of [5]. If we compare with existing commercial solutions of similar dimensions [8], [9], and assume our worst case (20×20 cm² plate), we achieved similar or even larger read ranges without making use of **expensive** ceramic substrates.

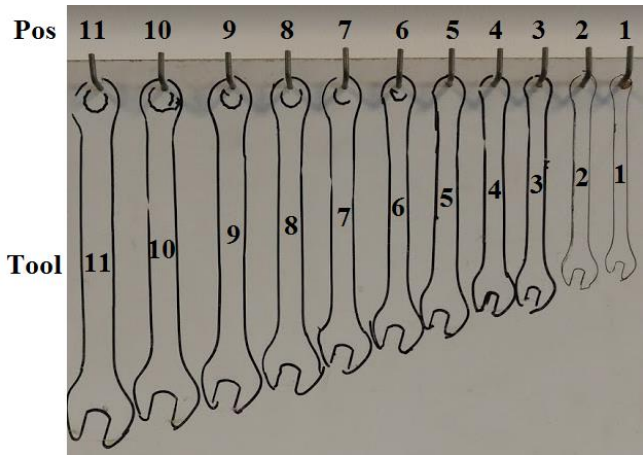


Fig. 11: Layout of the tool hanging board. Positions and tools have labelled from 1 to 11.

V. REAL SCENARIO MEASUREMENTS

The tool hanging board of Fig. 11 will be considered to evaluate the performance of the proposed design in a real multi-tag scenario. The length of the tools ranges from 10.5 cm to 19 cm whereas the width ranges from 0.5 cm to 1.5

cm. Spacing between tools ranges from 2 to 4 cm. In all the experiments, the distance between the reader and the board is 1 m in order to make sure that we can always read all tags.

A set of eleven antennas was fabricated and labelled (Fig. 12). Before soldering the AH4 chip we measured the power transmission coefficient **of each antenna** on a 20×20 cm² metal plate to assess the variations due to the fabrication process. Fig. 13 shows as, in the EU UHF band, we can expect **variations in the power transmission coefficient** smaller than 0.5 dB for most of the tags. Tag VIII is the worst case with a loss of 2.5 dB.



Fig. 12: Top view of the fabricated tags set.

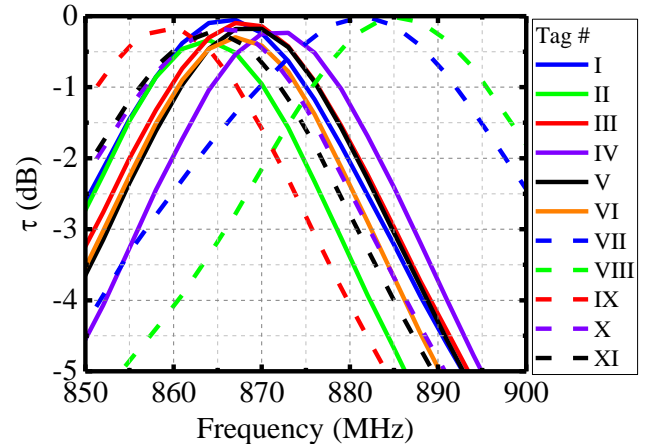


Fig. 13: Measured power transmission coefficient for the different tags of Fig. 12.

A. Experiment 1: effects of the tool size in the tag performance

In an initial experiment we considered the effect of the tool size in the performance of a tag. For this, we placed tag VI on each one of the tools and measured P_{to} with the tool, standing alone, in the center of the board (position 7 approximately). Fig. 14.a shows as P_{to} is minimum for tool 6 (length = 14.5 cm) and increases significantly for shorter

and longer tools. These results are in agreement with simulations of Fig. 6 and Fig. 7.

B. Experiment 2: variations of the tag realized gain due to fabrication issues.

The losses introduced in the antenna assembly will affect not only the power transmission coefficient but also the gain as well. For that reason, we designed an experiment to evaluate the variations of the realized gain $G\tau$. Fig. 14.b depicts the measured P_{to} for all the tags when they were placed on tool 7. In all cases, the tool was located in position 7. It can be seen as we can expect variations of ± 2.3 dB in P_{to} measurements due to the fabrication process.

C. Experiment 3: behavior of the tag for different observation angles

Next, we evaluate the behavior of the tag for different observation angles. In this experiment tag VI is placed again on tool 7. Then, P_{to} is measured when tool 7 is located in the different available positions of the board. Fig. 14.c shows as power required to activate the tag is smaller when it is at the edges of the board. Therefore, the size and shape of the tool has effects in the radiation pattern of the antenna, too.

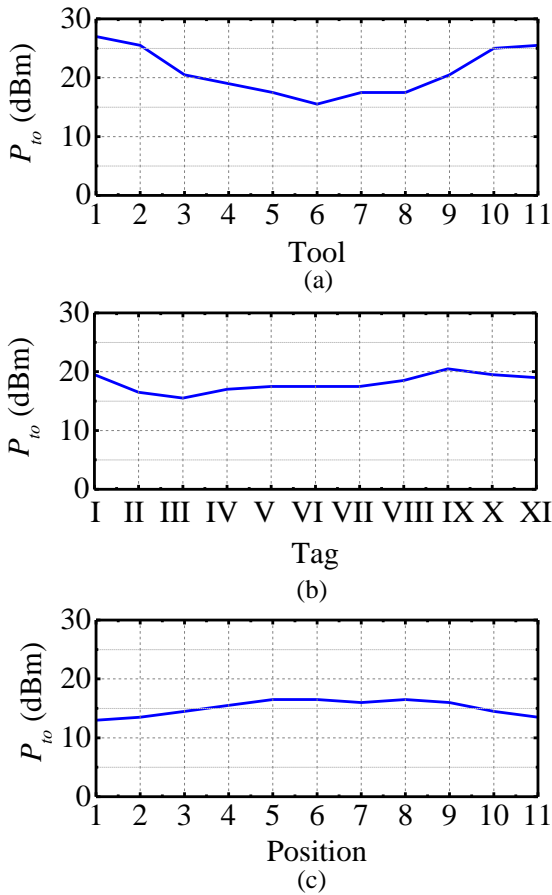


Fig. 14: a) Turn on power for tag VI when it is placed on different, standing alone, tools. Measurements were taken in position 7. b) Turn on power for all the tags when they are placed on tool 7. Tool 7 is located in position 7. c) Turn on power for tag VI when it is placed on tool 7. Tool 7 has been located in the different available positions of the board.

D. Experiment 4: performance of the tag in a full board

In this experiment, we placed each tag on its respective tool and situated the tool in its corresponding position. Firstly, we measured the P_{to} for each tag when the tool was standing alone in the board and, subsequently, the P_{to} for each tag when the board was full of tools (Fig. 15). Notice that the results for the stand alone scenario can be also obtained combining the effects illustrated in the previous three experiments. In the full board scenario, the P_{to} of all the tags is impaired (6.6 dB in average) due to the interactions with other tools that produce impedance mismatch and variations in the radiation pattern.

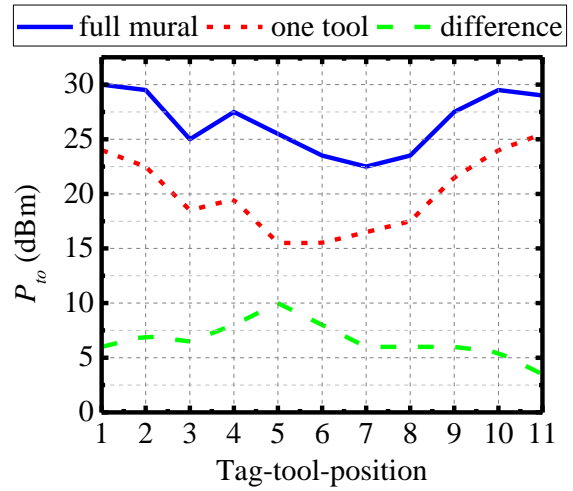


Fig. 15: Turn on power when every tag is placed in their respective tool and the tool is situated in its corresponding position.

VI. CONCLUSIONS

In this contribution, we presented a novel tag antenna design based on short-ended coupled patches operating in the EU UHF RFID band. **The antenna was miniaturized**, through a technique previously used for PIFA's, to obtain a reduced **volume (20 x 2.56 x 3 mm³)**, thus making it suitable for labelling metallic tools. Measurements in anechoic chamber showed that the fabricated prototype can attain a minimum read range of 3.3 meters on a variety of metallic plates of different sizes.

The dimensions of the metallic object being labelled have a relevant impact in the tag performance. We used simulations to demonstrate that the largest read range is expected for those dimensions that make the metallic plate resonant at the EU UHF RFID band.

We also assessed the tag performance in a real scenario: a tool hanging board with eleven wrenches of different sizes. Measurements confirmed the conclusions of simulations regarding the effects of the object size. They also showed that a significant impairment of the performance (**P_{to} decreased between 6-7 dB**) can be expected when the tag interacts not only with its own tool but with other tools in the vicinity, as well.

ACKNOWLEDGMENT

This work was supported by the Universitat Autònoma de Barcelona and the Spanish Ministerio de Economía y Competitividad and FEDER funds through project TEC2015-69229-R.

REFERENCES

- [1] E. Dovere, S. Cavalieri, S. Ierace, "An assessment model for the implementation of RFID in tool management", in *IFAC-PapersOnLine*, Volume 48, Issue 3, 2015, Pages 1007-1012.
- [2] X.L. Sui, Y. Teng, Y.Q. Chen, X.H. Wang, "Research on Application of RFID Technology in Tool Identification and Information Management", in *Advanced Science and Technology Letters* Vol.53 (AITS 2014), pp.353-356.
- [3] E. Valero, A. Adán and C. Cerrada, "Evolution of RFID Applications in Construction: A Literature Review", in *Sensors* 2015, 15, 15988–16008.
- [4] E.C. Jones, S. Gupta, L. Taylor Starr, "RFID Implementation and Enterprise Management in the Healthcare Sector", in *International Journal of Supply Chain Management*, Vol. 4, No. 3, September 2015.
- [5] T. Björninen, L. Sydänheimo, L. Ukkonen and Y. Rahmat-Samii, "Advances in antenna designs for UHF RFID tags mountable on conductive items," in *IEEE Antennas and Propagation Magazine*, vol. 56, no. 1, pp. 79-103, Feb. 2014.
- [6] F. L. Bong, E. H. Lim and F. L. Lo, "Flexible Folded-Patch Antenna With Serrated Edges for Metal-Mountable UHF RFID Tag," in *IEEE Transactions on Antennas and Propagation*, vol. 65, no. 2, pp. 873-877, Feb. 2017.
- [7] A. Hamani, M. C. E. Yagoub, T. P. Vuong and R. Touhami, "A Novel Broadband Antenna Design for UHF RFID Tags on Metallic Surface Environments," in *IEEE Antennas and Wireless Propagation Letters*, vol. 16, pp. 91-94, 2017.
- [8] (X1) Xerafy XS series, RFID on metal tags: <http://www.xerafy.com/userfiles/uploads/brochures/XS%20Brochure.pdf>.
- [9] (X2) William Frick & Company, metal mount tool tracking RFID tag: https://www.fricknet.com/Products/SmartMark_RFID/Metal_Mount_Tool_Tracking_RFID_Tag.html.
- [10] S. L. Chen and K. H. Lin, "A Slim RFID Tag Antenna Design for Metallic Object Applications," in *IEEE Antennas and Wireless Propagation Letters*, vol. 7, pp. 729-732, 2008.
- [11] S. L. Chen, "A Miniature RFID Tag Antenna Design for Metallic Objects Application," in *IEEE Antennas and Wireless Propagation Letters*, vol. 8, no., pp. 1043-1045, 2009.
- [12] S. L. Chen and R. Mittra, "A long read range RFID tag design for metallic objects," *Proceedings of the Fourth European Conference on Antennas and Propagation*, Barcelona, Spain, 2010, pp. 1-3.
- [13] K. H. Lin, S. L. Chen and R. Mittra, "A Looped-Bowtie RFID Tag Antenna Design for Metallic Objects," in *IEEE Transactions on Antennas and Propagation*, vol. 61, no. 2, pp. 499-505, Feb. 2013.
- [14] M. Polivka and M. Svanda, "Stepped Impedance Coupled-Patches Tag Antenna for Platform-Tolerant UHF RFID Applications," in *IEEE Transactions on Antennas and Propagation*, vol. 63, no. 9, pp. 3791-3797, Sept. 2015.
- [15] RongLin Li, G. DeJean, M. M. Tentzeris and J. Laskar, "Development and analysis of a folded shorted-patch antenna with reduced size," in *IEEE Transactions on Antennas and Propagation*, vol. 52, no. 2, pp. 555-562, Feb. 2004.
- [16] Alien Higgs-4, <http://www.alientechnology.com/products/ic/higgs-4>.
- [17] Arlon AD1000, <https://www.rogerscorp.com/documents/3269/acs/AD1000-Data-Sheet.pdf>.
- [18] FEKO EM Simulation software, <http://www.feko.info>.
- [19] G. Marrocco, "The art of UHF RFID antenna design: impedance-matching and size-reduction techniques", in *IEEE Antennas and Propagation Magazine*, vol. 50, no. 1, pp. 66-79, Feb. 2008.
- [20] X. Qing, C. K. Goh and Z. N. Chen, "Impedance Characterization of RFID Tag Antennas and Application in Tag Co-Design," in *IEEE Transactions on Microwave Theory and Techniques*, vol. 57, no. 5, pp. 1268-1274, May 2009.
- [21] Impinj, Speedway Revolution R220, <https://www.impinj.com/platform/connectivity/speedway-r220/> 2017.
- [22] Laird Technologies, S8658P, <https://www.lairdtech.com/products/s8658wpr> 2017.